UCRL-10106

University of California

Ernest O. Lawrence Radiation Laboratory

TWO-WEEK LOAN COPY

This is a Library Circulating Copy which may be borrowed for two weeks. For a personal retention copy, call Tech. Info. Division, Ext. 5545

Berkeley, California

DISCLAIMER

This document was prepared as an account of work sponsored by the United States Government. While this document is believed to contain correct information, neither the United States Government nor any agency thereof, nor the Regents of the University of California, nor any of their employees, makes any warranty, express or implied, or assumes any legal responsibility for the accuracy, completeness, or usefulness of any information, apparatus, product, or process disclosed, or represents that its use would not infringe privately owned rights. Reference herein to any specific commercial product, process, or service by its trade name, trademark, manufacturer, or otherwise, does not necessarily constitute or imply its endorsement, recommendation, or favoring by the United States Government or any agency thereof, or the Regents of the University of California. The views and opinions of authors expressed herein do not necessarily state or reflect those of the United States Government or any agency thereof or the Regents of the University of California.

Submitted for publication in Physical Review

UCRL-10106

UNIVERSITY OF CALIFORNIA

Lawrence Radiation Laboratory
Berkeley, California

Contract No. W-7405-eng-48

BREMSSTRAHLUNG FROM PROTON BOMBARDMENT OF NUCLEI

David Cohen, Burton J. Moyer, Harlan C. Shaw,
and Charles N. Waddell

September 19, 1962

Bremsstrahlung From Proton Bombardment of Nuclei

David Cohen, Burton J. Moyer, Harlan C. Shaw,
and Charles N. Waddell

Lawrence Radiation Laboratory
University of California
Berkeley, California

September 19, 1962

ABSTRACT

Various targets were bombarded with 38- to 185-MeV protons. Photons from these targets were viewed at experimentally available angles from the proton beam with a 180-deg pair spectrometer capable of detection in the photon energy range of 8 to 150 MeV. The accumulated spectra above 20 MeV, after subtraction of some π^0 photon contamination, are assumed to be due to proton bremsstrahlung. The general spectral features are explained in terms of electric-dipole radiation from p-n collisions, where the target neutrons are in motion. The detailed features are discussed in terms of the available theoretical predictions; there is good agreement with the phenomenological calculation using n-p scattering data.

Bremsstrahlung From Proton Bombardment of Nuclei*

David Cohen,† Burton J. Moyer, Harlan C. Shaw,‡
and Charles N. Waddell**

Lawrence Radiation Laboratory
University of California
Berkeley, California

I. INTRODUCTION

During the past several years there have been occasional efforts to study proton bremsstrahlung due to nuclear (noncoulombic) forces. These efforts have included both experimental determinations[1,2] and theoretical predictions.[3-12] Most of the theoretical work and all of the experimental work involved protons in the approximate energy range of 35 to 140 MeV. As proton energies increase above 140 MeV the bremsstrahlung spectra become masked by the greater photon intensity from π^0 production and decay, while somewhat below 25 MeV the photons from nuclear de-excitation obscure most of the bremsstrahlung spectral region.

Proton bremsstrahlung is of interest for evident reasons. It provides an indirect yet not highly sensitive way of gathering or confirming some information about nuclear forces. Also, it is occasionally desirable to know the photon spectra due to this process when other photon or nuclear processes are being investigated. For example, for confirmation of the existence of the π^0 meson by means of the photon decay spectra, it was necessary to estimate the nature of the contribution from proton bremsstrahlung.[13] Likewise in any investigation of radiative nuclear transitions induced by high-energy proton bombardment, the bremsstrahlung will underly the characteristic spectra.

This is a report of experimental work done during 1953 to 1955 at the 184-in. synchrocyclotron. Targets of various elements were bombarded

with the internal proton beam at various energies, and the photons from the target were viewed with a pair spectrometer from outside the shielding at certain available angles from the proton beam. There were two major restrictions: one was the low counting rate (occasionally as low as 1 cpm), and the other was the arrangement of the holes through the shielding wall, which restricted the possible combinations of proton energy and angle-of-view. In view of these restrictions, we measured only the spectra from the following bombardments:

(a) at 90 deg from the beam: 38-, 100-, and 140-MeV protons on beryllium;

(b) at 90 deg: 95-MeV protons on carbon, aluminum, and copper;

(c) at 2 and 178 deg: 185-MeV protons on beryllium, aluminum, and copper.

Spectral measurements were confined within the photon energy interval of about 8 to 150 MeV, although spectra below about 18 MeV are not analyzed here because of the presence of intense nuclear de-excitation photons whose treatment constitutes a separate problem.

The results may be compared with Wilson's previous experimental bremsstrahlung measurements;[1] our apparatus was designed to yield more accurate spectra than the absorption technique that he used. The results are also compared with theoretical predictions where possible; an extensive phenomenological calculation, soon to be published, has been performed by Beckham[12] and is specifically related to data such as these. In addition, some information is presented on π^0 production near threshold, since the spectra from 185-MeV protons contained photons resulting from this process.

II. EXPERIMENTAL PROCEDURES

A. Cyclotron Facilities

Figure 1 shows the experimental arrangement. In all cases the pair spectrometer was outside the concrete shielding at a typical distance of 50 ft from the targets. For measurements at 90 deg the targets were viewed through a hollow radial probe, and the energy of the incident beam was changed by moving the targets to different radii.

The study of the angular distribution of the bremsstrahlung was limited to three angles--2, 90, and 178 deg--and at 2- and 178-deg to a single proton energy (185 MeV) by the availability of cyclotron tank windows, target-support probes, and holes through the concrete shielding. For the 2- and 178-deg measurements the spectrometer was placed at a position that permitted the choice of viewing the targets at the 185-MeV radius or at the 340-MeV radius by slight rotation of the spectrometer magnet. This permitted testing the spectrometer electronics with the reasonably intense beam of photons resulting from the decay of the π^0 mesons. The direction of the cyclotron magnetic field was reversed to change the viewing angle from 2-deg to 178-deg. For the 2-deg measurements collimators were necessary inside the holes through the concrete to reduce the background activity of the spectrometer counters produced by the forward neutron flux from the target.

B. Pair Spectrometer

The pair spectrometer used in this experiment was of the 180-deg type, and was designed to measure gamma rays in the 8 to 150-MeV range. A diagram of the apparatus is shown in Fig. 2. Since the counting rates and background encountered in this experiment were typically low, Geiger tubes could be used to detect the magnetically analyzed pair partners and

thus simplify the electronics. A 180-deg geometry was chosen to minimize the effects of the angular divergence of the pair partners on the resolving power of the instrument. Since thin converters were used, the spectrometer chamber and a 6-ft-long region in front of the converter were evacuated in order to eliminate pair production in the air. An 18-in. collimator was built into the evacuated brass pipe, and a magnetic clearing field was provided to eliminate pairs formed in the entrance foil and the collimator.

For a given magnetic field, all coincidences between pairs of counters having the same physical separation were produced by gamma rays of the same energy. The Geiger pulses resulting from an electron-positron pair were changed to 1-μsec pulses and fed to a coincidence circuit; however, if two or more Geiger tubes in either one of the banks fired within 1 μsec, an anticoincidence pulse was generated that eliminated the output of the coincidence circuit. The two-fold coincidence output initiated a gate which was fed to the Geiger-tube amplifiers, allowing them to register any events occurring within the resolving time of the coincidence circuit.

Ten Geiger tubes were used in each of the two banks of detectors, giving in all 100 possible coincidence pairs. The recording of the coincidence pairs into 19 energy channels was accomplished by use of a 10-element square matrix consisting of 100 coincidence circuits. The outputs of the energy channels and the counts from each Geiger tube were registered. This system is similar to that used by R. L. Walker and B. D. McDaniel,[14] and a more detailed description of the electronics used will be found in references 2 and 15. The detectable photon energy ranges within an 8 to 150-MeV interval were varied by changing the magnet current, allowing overlapping spectra.

The spectrometer was calibrated and the focusing properties checked by use of the floating-wire technique. The results of this calibration were

checked against the orbits calculated from the magnetic field distribution measured by means of a proton spin-resonance probe. These calibrations were independently verified by observing the 17.64-MeV gamma ray from Be^{8*} produced at the 440-keV resonance of the $Li^7(p, \gamma)Be^8$ reaction,[16] and the 15.11-MeV gamma ray produced in the $C^{12}(p, p')C^{12*}$ reaction.[15, 17] The agreement between these calibrations was within the energy width of a channel, that is, about 4%.

The resolution of a pair spectrometer of this type is essentially determined by three factors: (a) the finite width of the counters, (b) multiple scattering in the converter, and (c) radiation straggling of the pair members in the converter. The channel width from (a) gives rise to a triangular resolution function with a full width at half maximum of 5% for the median energy channel. Multiple scattering (b) only had a small effect on the resolution, and only at the lowest gamma-ray energies (8 to 15 MeV) because of the thin converters and the 180-deg geometry. Radiation straggling (c) was insignificant, since the thickness of the converters was less than 0.02 radiation lengths.

The efficiency of the spectrometer is determined by (1) the pair-production cross section, (2) the fraction of the pairs with a division of energy in the detectable interval, (3) vertical scattering in the converter, and (4) the leakage of particles between Geiger tubes. Items (1) and (2) were evaluated by integration of the differential pair-production expression as given, for example, by Rossi and Greisen,[18] between the limits of the energy-division parameter μ, for the pair energy W, which are allowed by the geometry. Figure 3 illustrates this process. Item (3) was calculated by numerical integration, and was found to be independent of channel number for a given converter thickness and magnetic-field setting. The losses were kept reasonably small by the use of thin converters of high Z. Item (4) was

evaluated from geometrical considerations. The efficiency calculations were empirically checked by measuring the counting rate as a function of converter thickness for photons of differing energies. The observed spectra were also measured with magnetic-field settings that gave overlapping energy ranges to minimize uncertainties from Geiger tube efficiencies.

C. Beam Monitoring

The cyclotron internal beam current was determined from a measurement of the amount of thermal power generated in the target during bombardment. The targets were clamped to the end of a thin copper bar which was extended radially into the cyclotron tank, and the entire unit was bolted to the water-cooled end of the probe. Constantan wires soldered to both ends of the copper bar permitted measurement of the temperature difference resulting from the flow of heat down the copper bar. This thermocouple arrangement was calibrated by substituting a resistor for the target and measuring the differential thermal electromotive force for various input power levels. The radiation loss was evaluated by measuring the thermal decay curves for various targets bombarded to different initial temperatures. For lower beam currents the decay curve was exponential, and a small deviation was noted for metal targets bombarded with the full cyclotron beam. This deviation was more marked for a carbon target. From the analysis of the decay curves the radiation loss obtained with each target could be evaluated. Confidence in this evaluation was obtained from the reproducibility of data taken at various beam levels.

From the data taken with the metallic targets it was found that, for a given spectrometer position and collimator arrangement, the singles counting rates of the Geiger tubes provided a reliable monitor of the number of γ rays produced at the target. Thus it proved possible to calibrate the singles counting rates at a low beam level and to use the counting rates as a monitor for higher beam levels, where radiation losses were significant.

D. Plotting of the Data

Experimental results are shown in Figs. 4 through 9. The vertical bars denote probable errors; they include both the statistical errors and occasional systematic errors, whenever these could be identified.

The photon spectra within the 8- to 150-MeV energy span were obtained by using five settings of the magnetic field. Because of the low counting rates, it was usually necessary to accumulate data at each magnetic-field setting for several hours. The magnetic-field settings were cycled so that the data for each setting were accumulated in several runs separated by some hours of running time. A comparison of these yields served as a check on the reproducibility of the data.

The raw spectrometer data were first corrected for counting losses and accidental counts, and then the efficiency correction was applied to each channel. In energy intervals where the cross sections vary slowly with photon energy, the data for several channels were combined to reduce statistical errors. The data from each magnetic-field setting were treated independently, and the agreement in the overlap regions gave confidence as to the validity of the data and its treatment.

III. RESULTS AND DISCUSSION

A. Photons from Nuclear De-excitation

In the low-energy region of the spectra, for $k \lesssim 20$ MeV, radiative de-excitation of residual nuclei will contribute photons in addition to those produced by proton bremsstrahlung. For excitation energies less than the threshold for particle emission, only radiative decay is possible, but for higher excitation energies, the radiation width is small compared to the particle widths. For example, for medium-weight nuclei the neutron width Γ_n is found to be about 10^3 to 10^4 times the radiative width Γ_γ near the neutron threshold, though the charged-particle widths are of course suppressed for outgoing particles with energy less than the Coulomb-barrier energy.[19] The angular distribution of photons emitted from the continuum of states will be symmetric about 90 deg because of averaging over states of even and odd parity.

The lower-energy photon spectra measured at 2 deg and 178 deg with respect to the beam direction from the bombardment of Al with 185-MeV protons are shown in Fig. 4. The cross sections for the 2-deg spectrum have been increased by a factor of 10 to separate the curves, and the dashed straight lines represent the same cross section for the two spectra. The intensity of the radiation decreases exponentially with increasing photon energy, and a sudden change in the yield curve occurs at $k \sim 12$ MeV. Comparison with the dashed line shows that there is fore-aft symmetry in the laboratory system for photons with $k \lesssim 12$ MeV, and that the higher-energy photons show the forward peaking in the laboratory system expected from proton bremsstrahlung.

The spectra obtained in the bombardment of Be, C, and Cu targets exhibit the same kind of features as the Al spectra. The discontinuity in yield occurs at $k \approx 10$ MeV for Be^9, $k \approx 9$ MeV for C^{12}, and at $k \approx 12$ MeV for Cu. In addition, the previously reported 15.11-MeV gamma ray is

observed superimposed on the bremsstrahlung spectrum in the bombardment of C^{12}.[16, 17] In the bombardment of Be^9, gamma rays of approximately 14 and 18 MeV are observed, presumably resulting from the radiative decay of the 17.6-MeV level of Be^{8*} produced in the (p, pn) or (p, d) reactions.[16]

Since a number of residual nuclei are produced in the proton bombardment of these targets, and each residual nucleus has a somewhat different threshold for particle emission, there is an energy range in which the break in the photon yield curve would be expected to occur. In each case the energy of the observed break is found to be within the expected range, and, in fact, it occurs at nearly the highest expected value. This fact and the nature of the angular distributions are consistent with the interpretation that the lower-energy photons result from nuclear de-excitation and the higher-energy photons ($k \gtrsim 20$ MeV) are from proton bremsstrahlung.

B. π^0 Meson Production near Threshold

The data from 185-MeV protons on Be, given in Fig. 5, show clear evidence of a contribution of photons from π^0 decay superimposed upon a bremsstrahlung yield. This is most pronounced in the 2-deg curve of Fig. 5, which displays a curve with downward concavity in the general region from 60- to 120-MeV photon energy, in marked contrast to the character of the spectrum curves of Figs. 6 and 7.

A rough quantitative separation of the π^0 photon spectrum from the bremsstrahlung for the 2- and 178-deg data of Fig. 5 was accomplished by using the following considerations:

(a) Energy limits to the π^0 spectrum can be calculated kinematically if we assume reasonable production reactions, such as $Be^9 + p \rightarrow Be^8 + p + n + \pi^0$. Thus we find that in the forward direction (2 deg) the π^0 photons will lie between 38 and 140 MeV, while in the backward direction (178 deg) the limits will be 32 and 120 MeV.

(b) If the π^0 production occurs predominantly in a reference frame moving with relative velocity β in a direction parallel to the incident protons, the forward and backward π^0 photon spectra are related by

$$F(k, 0 \text{ deg}) = \frac{1+\beta}{1-\beta} \; F(\frac{1-\beta}{1+\beta} k, \; 180 \text{ deg}),$$

where F signifies photons/sr-MeV.

(c) The characteristic spectrum shape for the bremsstrahlung was assumed to be similar to that in Fig. 7, but with a higher upper limit for the energy.

(d) It was found possible to subtract estimated bremsstrahlung curves, indicated in Fig. 5, from the 2- and 178-deg data so as to leave the remaining π^0 photon spectra that were related by the transformation mentioned above in (b) for a value of $\beta = 0.21$. This value of β corresponds to a collision frame for a 185-MeV proton and a counter-moving 20-MeV nucleon (neutron) in the Be nucleus.

Such an analysis leads to a total π^0 production cross section of about 4 μb per Be nucleus. This value is compatible with the extrapolation downward to 185 MeV of the π^0 yield curve vs proton energy given in Ref. 20 (for the carbon nucleus). It is likely that the data in that reference possess an unidentified background which causes its low-yield point to fall considerably too high, above the yield curve fitted to the data at the higher energies.

No attempt was made to analyze the spectra from Al and Cu targets, because of poor statistics and the complications of multiple nucleon collisions.

C. Bremsstrahlung Identification and Spectral Features

For the spectral region at energies greater than about 20 MeV, except for the π^0 photons produced in the case of 185-MeV incident protons, the photon yield is considered to be entirely due to proton bremsstrahlung. This conclusion is based upon the following considerations:

1. Photon emission at such energies cannot compete with particle emission as a process of nuclear de-excitation, but even more certainly

the forward-to-backward yield ratio of the non-π^0 photons seen in Fig. 8 cannot be accounted for in terms of nuclear gamma radiation. The kinematics do not allow a motion of an excited nuclear system with sufficient velocity relative to the laboratory reference frame to give Doppler-shift effects of this magnitude. Doppler shift and aberration will account for the forward-backward effect, however, if the radiation originates in the center-of-mass frames of incident protons in collision with individual nucleons of the target.

2. The experimental cross sections and spectral shapes in Figs. 5, 6, and 7 (except for the π^0 yield in the first) agree roughly with phenomenological calculations of bremsstrahlung from p-n collisions.[4, 12]

In justification of the p-n collision origin, rather than a p-nucleus origin, we refer to the fact that for a 140-MeV proton the value of $\lambda\!\!\!^{-}$ is about 0.4 fermis, which is an order of magnitude smaller than the Be nuclear diameter. The impulse approximation model has been used with adequate success even at energies below 100 MeV,[21] and it is assumed to apply here. Only p-n collisions will significantly contribute, since p-p collisions provide no dipole radiation at energies where only elastic processes occur.

Certain factors, however, modify this simple p-n collision model, which may be identified as follows:

a. The neutron momentum distribution in the nucleus precludes the existence of a unique reference frame for the origin of the bremsstrahlung. Doppler shifts and aberrations of solid angle are thus not simple and unique in their effect upon the relation between the laboratory spectra and the p-n collision radiation. Also the p-n collision cross section varies quite rapidly as a function of relative velocity in this energy region.

b. Multiple collisions within a given nucleus are not negligible. By reference to the p-n and p-p collision cross sections at various energies, and with some allowance for the effect of the Pauli principle, we estimate

the probability of more than one collision in the traversal of a Be nucleus by a 140-MeV proton to be 0.4. In the cases of 100- and 40-MeV protons this probability is 0.5 and 0.8, respectively. The principal effect of such multiple collisions is a reduction in the mean nucleon collision energy. This effect is slight in the 140- and 100-MeV cases, but is considerable at proton energies as low as 40 MeV. For target nuclei such as Al and Cu, multiple collisions must be a dominant situation; indeed, it is likely that in such cases the correct model for the bremsstrahlung process would be more like the collision of the proton with the complex potential well of the nucleus, as treated in Ref. 10.

c. The Pauli principle will suppress the spectral yield at the high-energy end to some degree, as Beckham has pointed out in his calculation.[12]

In Fig. 8 are presented 90-deg data from the bombardment of Be by 38-, 100-, and 140-MeV protons. Here the ordinate is $k\, d^2\sigma/d\Omega dk$, so that a $1/k$ spectral characteristic would appear as a horizontal line. The curves for 100 and 140 MeV are derived from the curves of Figs. 4 and 5, without acknowledging the errors. They suggest a region of $1/k$ behavior followed at higher energies by a tailing off due to the nucleon momentum distribution. The 38-MeV curve is influenced over its entirety by the momentum distribution and by the effect of multiple collisions.

A comparison of the spectra from different elements at 90-deg for incident 95-MeV protons is shown in Fig. 9. The increasing relative enhancement of yield at low energies as the atomic number of the target is raised indicates the effect of multiple collisions. Not displayed are some data at 2 deg and 178 deg for Cu and Al for 185-MeV protons; in these the forward-to-backward yield ratio is greatly reduced from that appearing in the case of Be. Thus the quasi-free p-n collision model is not appropriate to the larger nuclei.

IV. COMPARISON WITH THEORETICAL PREDICTIONS

The theoretical predictions that have been published or are available to us can be divided into three categories:

1. treatment of the nucleus as a whole, by using the optical model,[10]
2. bremsstrahlung from pure nucleon-nucleon collisions,[4,7,8,9,11]
3. bremsstrahlung from p-n collisions where the neutrons exist within the nuclear matter.[2,12]

The optical-model calculation[10] was not carried out to the point where the results could be compared with experimental results; computing-machine calculations would be necessary.

A comparison of predictions from category 2 with experimental results is difficult because of the large spectral effects depending upon momentum distributions, multiple collisions, the exclusion principle and the existence of target nucleons within nuclear matter. However, there are some features of some of the predictions which are not completely obliterated by these three factors, and comparison with these features is possible.

The calculation using pseudoscalar theory with pseudoscalar coupling[7] is completely ruled out, because it predicts a $k(T^* - k)^{1/2}$ spectral shape and a $(T^*)^2$ dependence, where T^* is the available energy in the center of mass of the collision. The calculation using scalar meson theory with scalar coupling[7] is also completely ruled out because it predicts a 90-deg/0-deg flux ratio of 230. The phenomenological calculation[4] yields an approximately correct spectral shape $k^{-1}(T^* - k)^{1/2}$, total cross section σ, and energy dependence of $(T^*)^{-1}$; it is not possible to compare the angular distribution.

The predictions from category 3 do lend themselves to clear comparison with experiment. The treatment[2] of phenomenological results[4] combined with momentum distribution will not be discussed, since it is a special case of Beckham's[12] more general treatment with machine computations.

Beckham used the Born approximation and the phenomenological radial square-well potential of $V = V_0 [a + (1 - a)P_m] + V_\delta$, where V_0 is the well depth, P_m is the exchange operator, a is the parameter $(0 \leq a \leq 1)$ denoting the relative strength of the exchange operator, and V_δ is a repulsive core. Parameters in the above expression were varied until there was a fit with n-p elastic-scattering data at 100 MeV. The procedure was repeated at 180 MeV, and an interpolation made for 140 MeV. The exclusion principle, which forbids certain final states, produced an effect that depended upon the momentum distribution chosen.

The momentum distribution was then varied in an attempt to make the transformed spectra match the spectra of Figs. 5, 6, and 7. It was not possible to match the absolute yield data without decreasing V_0 by about 25% from the value originally chosen for the n-p scattering fit, but by this means a good match with experimental curves was obtained. Because of the difficulties of absolute measurement of the circulating proton beam at the target, this adjustment of V_0 is not felt to be significant. The calculated spectra were sensitive to the choice of repulsive core, and strongly sensitive to the choice of momentum distribution. The anticipated publication by Beckham[12] will present such features quantitatively.

ACKNOWLEDGMENTS

The authors are indebted to Mr. James Vale and Mr. Lloyd Hauser for their help in organizing and maintaining the runs, and to the cyclotron crew, maintenance men, and many other divisions of the Laboratory who contributed to this experiment. We especially wish to thank Colonel Beckham for allowing us to quote some of his thesis results, and for his help and suggestions during many discussions.

FOOTNOTES AND REFERENCES

*This work was performed under the auspices of the U. S. Atomic Energy Commission.

†Now at the Argonne National Laboratory, Argonne, Illinois.

‡Now at Tracerlab, Inc., Richmond, California.

**Now at the Physics Department, University of Southern California, Los Angeles, California.

1. R. Wilson, Phys. Rev. 85, 563 (1952).

2. David Cohen, Ph. D. thesis, Lawrence Radiation Laboratory Report UCRL-3230, December, 1955 (unpublished). The present work is an extension of this thesis, which dealt with only the spectra at 90 deg.

3. S. Hayakawa, Phys. Rev. 75, 1759 (1949).

4. J. Ashkin and R. E. Marshak, Phys. Rev. 76, 58 (1949).

5. I. Pomeranchuk and I. Shmushkevich, Dokl. Akad. Nauk. SSSR 64, 499 (1949).

6. G. Avak'iants, Zh. Eksperim. i Teor. Fiz. 20, 944 (1950).

7. A. Simon, Phys. Rev. 79, 573 (1950).

8. B. L. Timan, Soviet Phys. JETP (English transl.) 3, 711 (1956).

9. R. E. Cutkosky, Phys. Rev. 103, 505 (1956).

10. B. Kursunoglu, Phys. Rev. 105, 1846 (1957).

11. C. Dullemond and J. J. de Swart, Physica 26, 664 (1960).

12. Private communication from Col. Walter C. Beckham (USAF), Lawrence Radiation Laboratory, Livermore, California, who has recently completed computations of proton bremsstrahlung spectra for his doctoral thesis.

13. R. Bjorklund, W. E. Crandall, B. J. Moyer, and H. F. York, Phys. Rev. 77, 213 (1950).

14. R. L. Walker and B. D. McDaniel, Phys. Rev. 74, 315 (1948).

15. Charles N. Waddell, Ph. D. thesis, Lawrence Radiation Laboratory Report UCRL-3901, August 13, 1957 (unpublished).

16. F. Ajzenberg-Selove and T. Lauritsen, Nucl. Phys. 11, 1 (1959).

17. D. Cohen, H. C. Shaw, B. J. Moyer, and C. N. Waddell, Phys. Rev. 96, 714 (1954).

18. B. Rossi and K. Greisen, Rev. Mod. Phys. 13, 240 (1941).

19. J. M. Blatt and V. F. Weisskopf, Theoretical Nuclear Physics, (John Wiley and Sons, Inc., New York, 1952) Chaps. 2 and 9.

20. W. E. Crandall and B. J. Moyer, Phys. Rev. 92, 749 (1953).

21. J. W. Meadows, Phys. Rev. 98, 744 (1955).

FIGURE LEGENDS

Fig. 1. Plan view of experimental arrangement.

Fig. 2. Plan view of the 180-deg pair spectrometer.

Fig. 3. Diagram illustrating how the detection efficiencies of channels of constant energy were calculated. The geometric efficiencies, which are proportional to the fraction of pairs which could possibly be intercepted by the detection geometry, were multiplied by the areas under "flattened" splitting curves.

Fig. 4. Low-energy photon spectra from 185-MeV protons on aluminum, at 2 deg and 178 deg from the proton beam. The cross sections for the 2-deg spectrum have been increased a factor of ten to separate the curves, and the dashed straight-lines represent the same cross section for the two spectra. These spectra have not been corrected for spectrometer line shape; this correction would slightly increase the cross section at the lowest photon energies.

Fig. 5. Photon emission from 185-MeV protons on beryllium, at 2 deg and 178 deg from the proton beam. (A) Curve fitted to 2-deg data; (B) curve fitted to 178-deg data; (C) estimated curve for pure bremsstrahlung at 2 deg; (D) estimated curve for pure bremsstrahlung at 178 deg. (See text, Sec. III. B for discussion of these curves.)

Fig. 6. Photon emission at 90 deg from 100-MeV protons on beryllium. Nuclear de-excitation photons are present for $k < 18$ MeV.

Fig. 7. Photon emission at 90 deg from 140-MeV protons on beryllium. Nuclear de-excitation photons are present for $k < 18$ MeV.

Fig. 8. Energy emission spectra from Be target at 90 deg as a function of proton bombarding energy. Curves labeled 100 and 140 are reproduced from the smooth curves of Figs. 6 and 7. Note that here we plot $k\, d^2\sigma/d\Omega dk$. The numbers on the curves give proton energies in MeV.

Fig. 9. Photon spectra at 90 deg from 95 MeV protons on carbon, aluminum, and copper. The lowest curve (from 100-MeV protons on beryllium) is reproduced from Fig. 6.

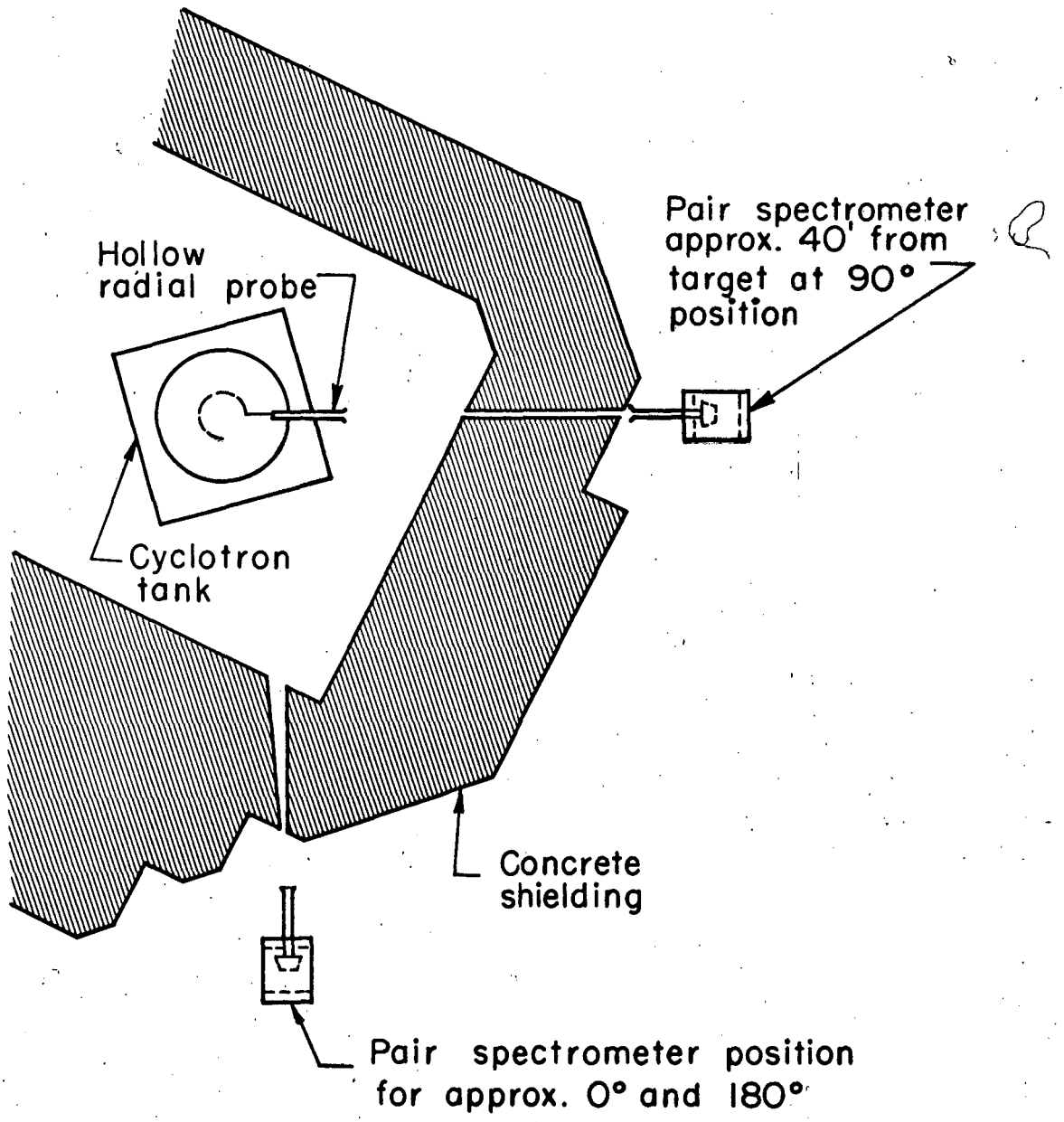
Pair spectrometer approx. 40' from target at 90° position
Hollow radial probe
Cyclotron tank
Concrete shielding
Pair spectrometer position for approx. 0° and 180°
MU-28368

Fig. 1

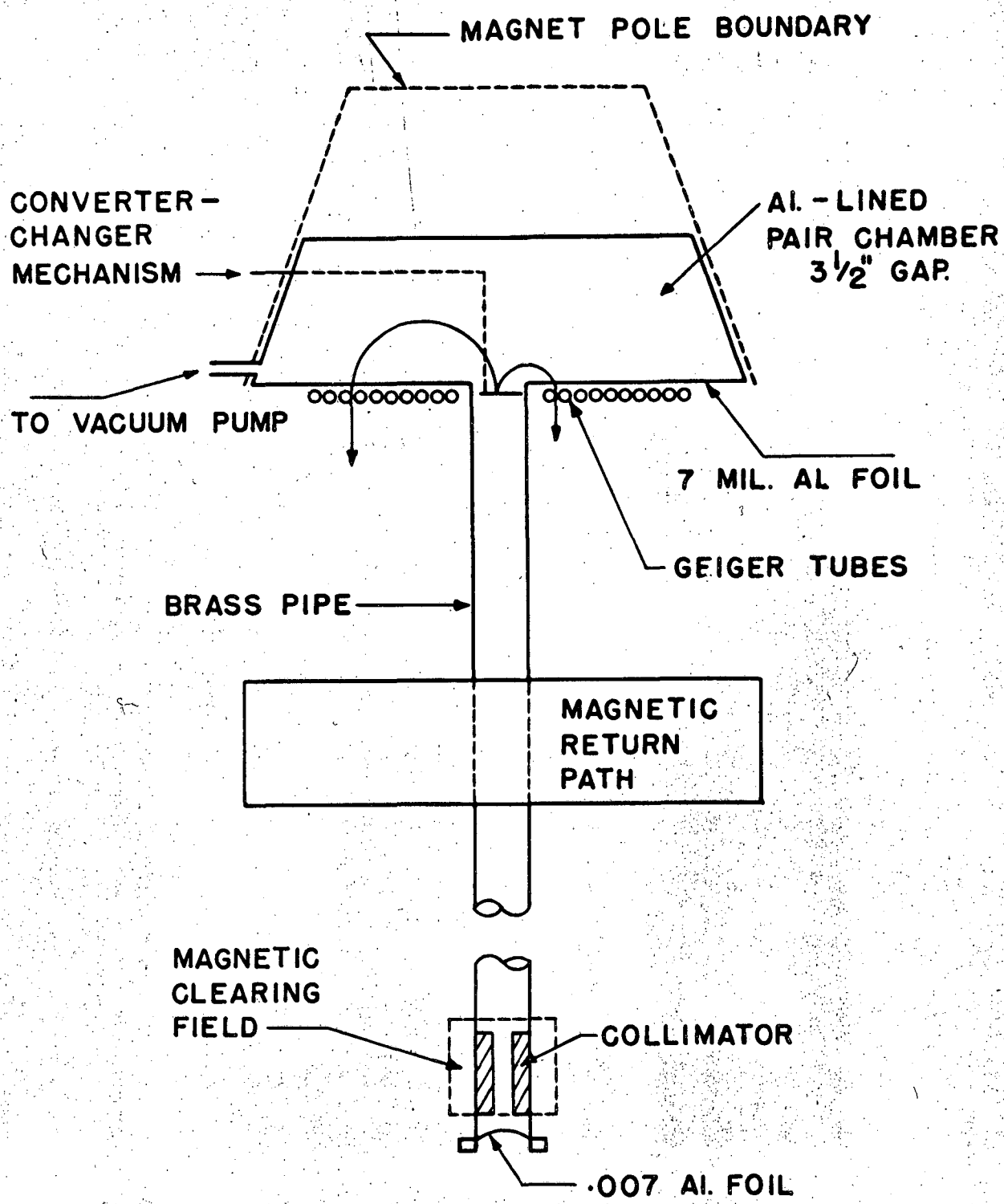

MU-10536

Fig. 2

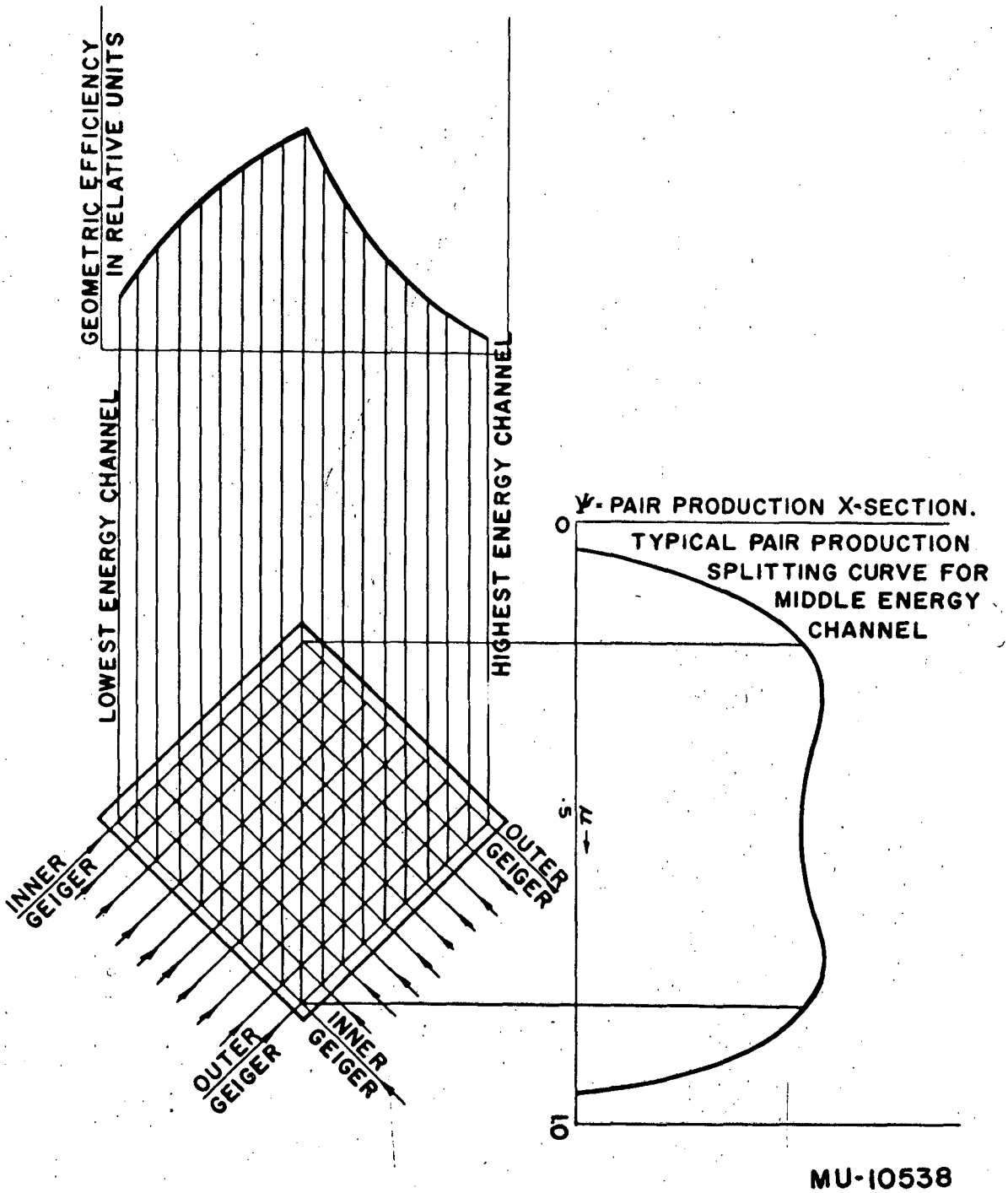
GEOMETRIC EFFICIENCY
IN RELATIVE UNITS
LOWEST ENERGY CHANNEL
HIGHEST ENERGY CHANNEL
INNER GEIGER
OUTER GEIGER
OUTER GEIGER
INNER GEIGER
Ψ- PAIR PRODUCTION X-SECTION.
TYPICAL PAIR PRODUCTION SPLITTING CURVE FOR MIDDLE ENERGY CHANNEL
0
1.0
s
MU-10538

Fig. 3

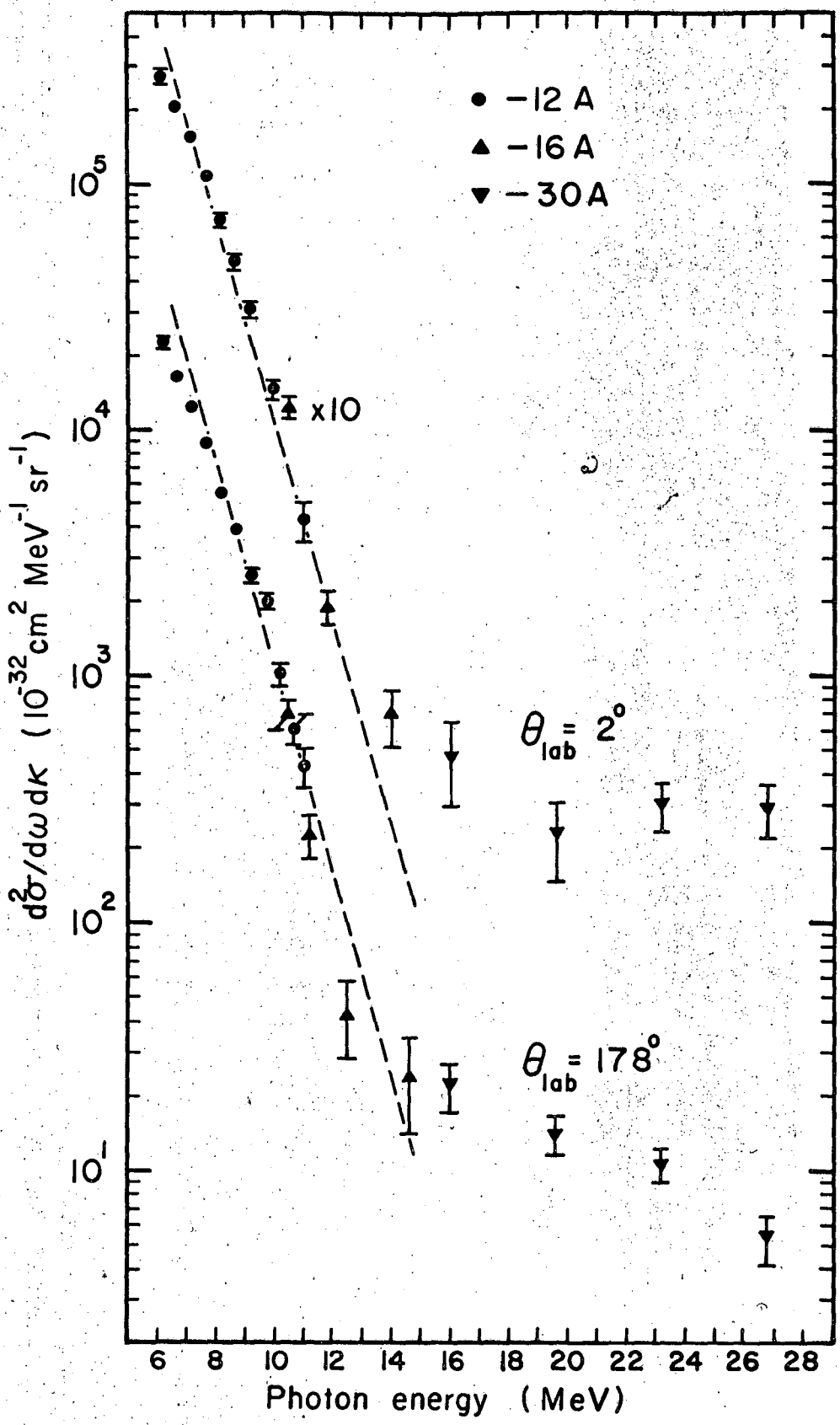

MU-28309

Fig. 4

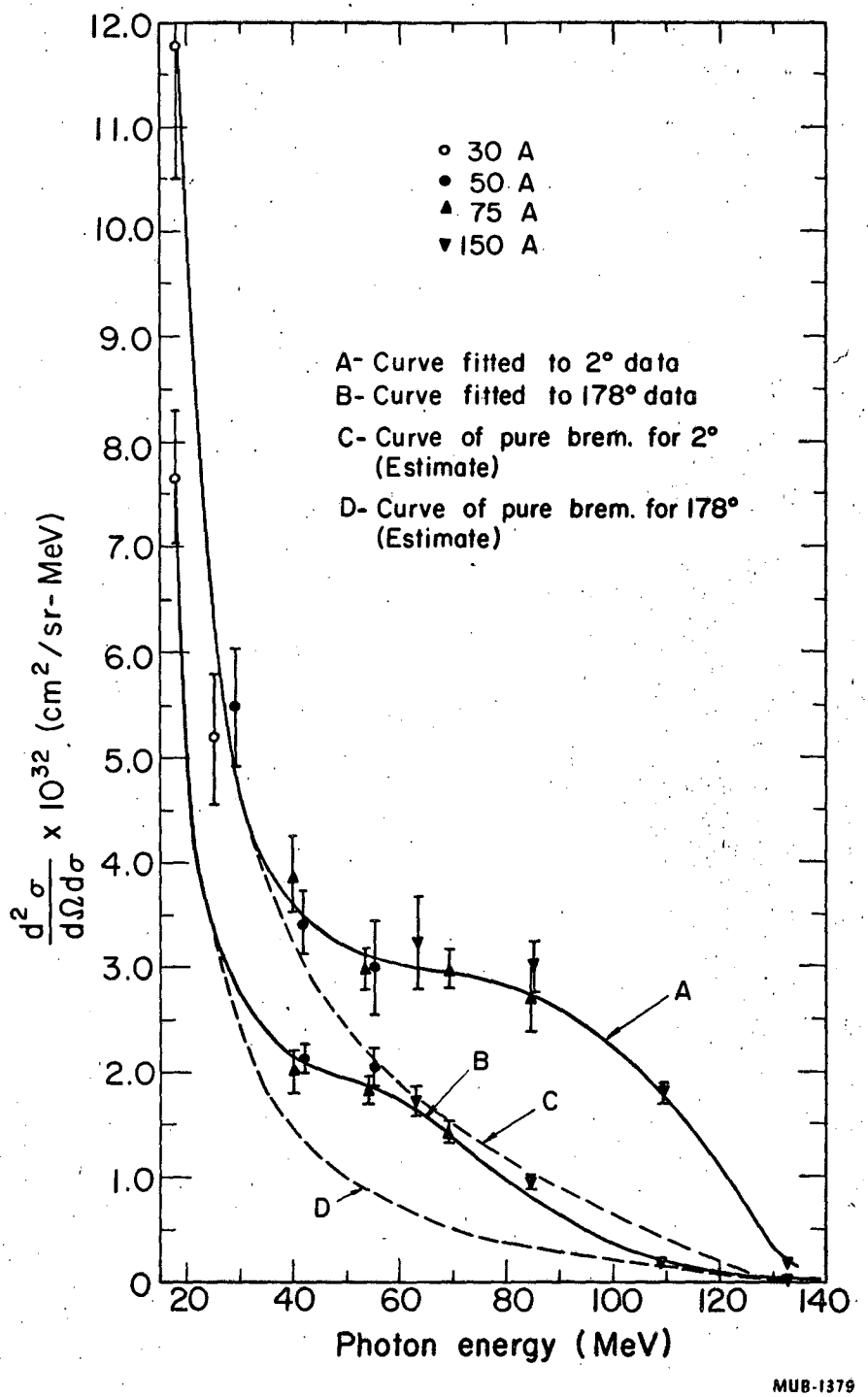
12.0
11.0
10.0
9.0
8.0
7.0
6.0
5.0
4.0
3.0
2.0
1.0
0
20
40
60
80
100
120
140
Photon energy (MeV)
$\frac{d^2\sigma}{d\Omega d\sigma} \times 10^{32}$ (cm^2/sr-MeV)
30 A
50 A
75 A
150 A
A- Curve fitted to 2° data
B- Curve fitted to 178° data
C- Curve of pure brem. for 2° (Estimate)
D- Curve of pure brem. for 178° (Estimate)
A
B
C
D
MUB-1379

Fig. 5

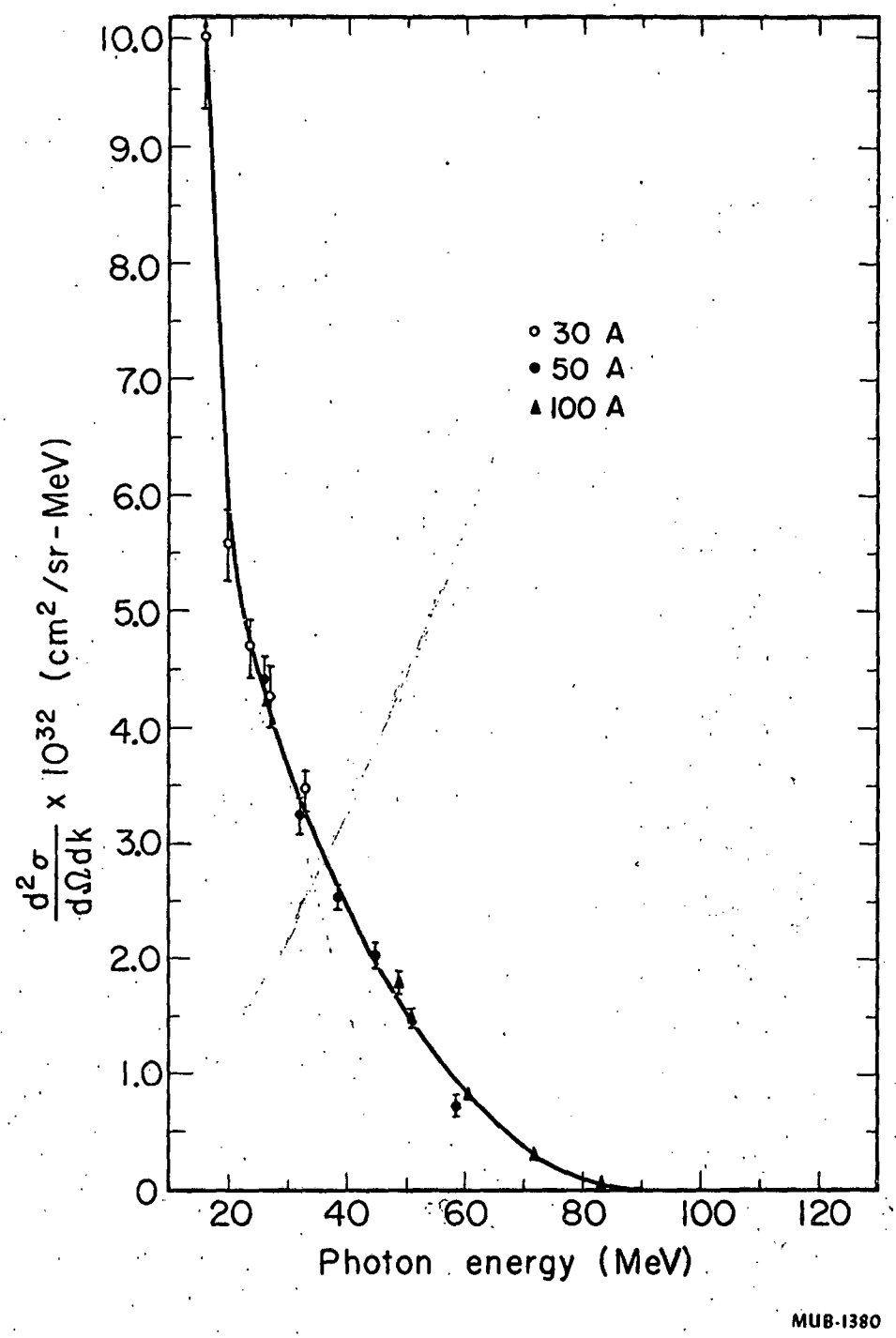
10.0
9.0
8.0
7.0
6.0
5.0
4.0
3.0
2.0
1.0
0
20
40
60
80
100
120
Photon energy (MeV)
$\frac{d^2\sigma}{d\Omega dk} \times 10^{32}$ (cm^2/sr-MeV)
○ 30 A
● 50 A
▲ 100 A
MUB-1380

Fig. 6

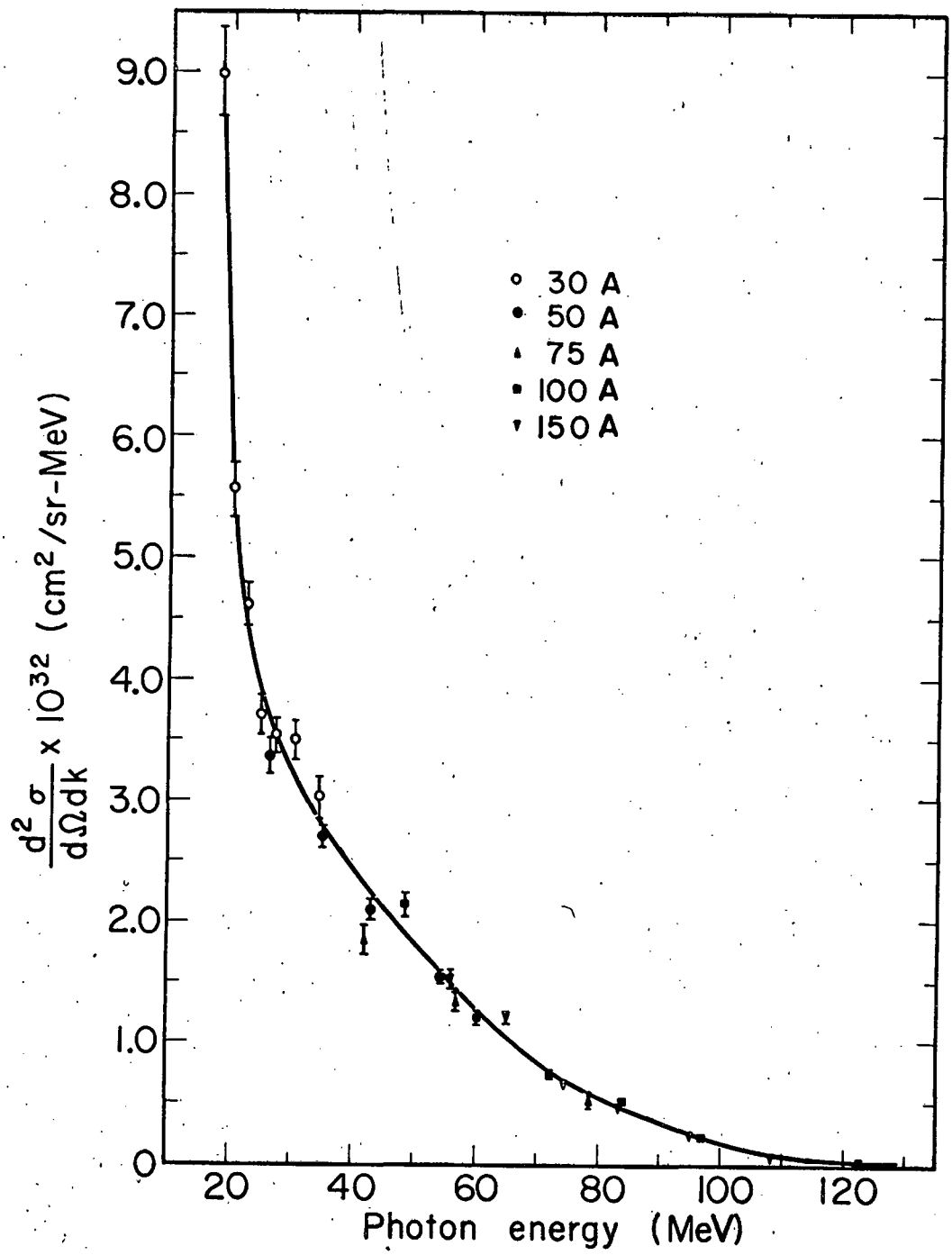

MUB-1381

Fig. 7

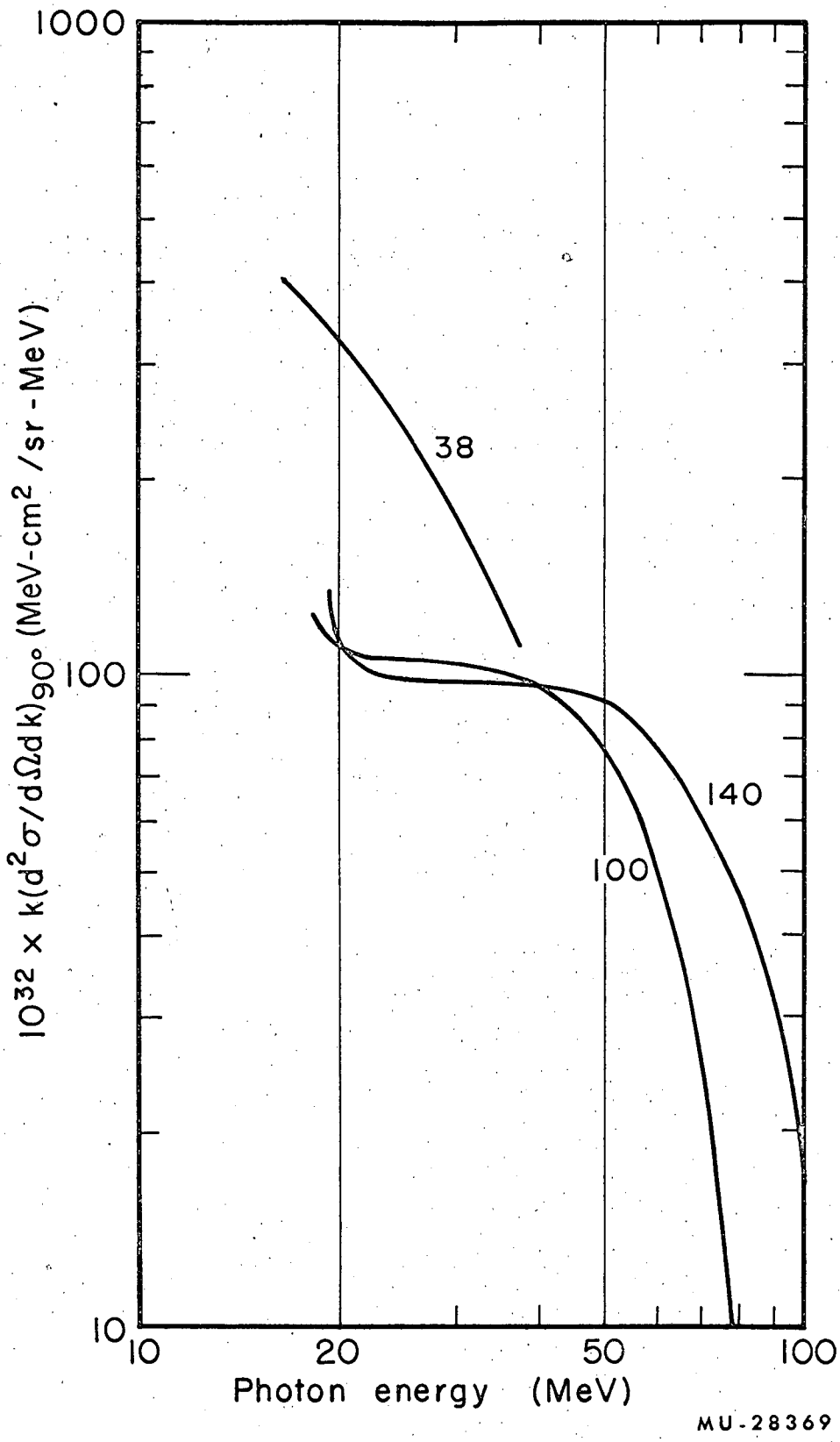
1000
100
10
10
20
50
100
Photon energy (MeV)
$10^{32} \times k(d^2\sigma/d\Omega dk)_{90°}$ (MeV-cm^2/sr-MeV)
38
140
100
MU-28369

Fig. 8

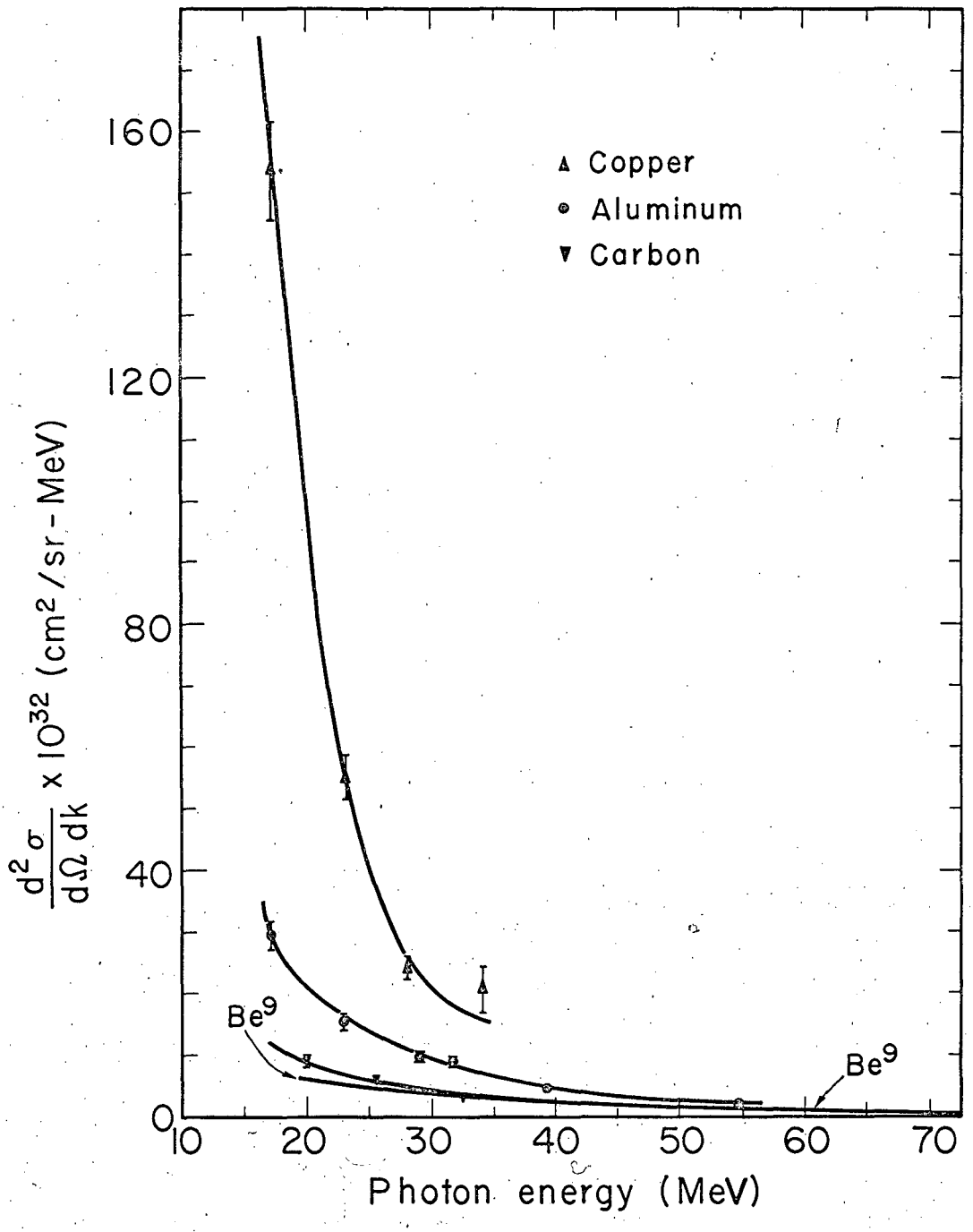

MUB-1382

Fig. 9